

---

# Med-R1: Reinforcement Learning for Generalizable Medical Reasoning in Vision-Language Models

---

Yuxiang Lai<sup>1\*</sup> Jike Zhong<sup>2\*</sup> Ming Li<sup>3\*</sup> Shitian Zhao<sup>4</sup> Xiaofeng Yang<sup>1,5,6†</sup>

<sup>1</sup>Department of Computer Science and Informatics, Emory University

<sup>2</sup>Department of Computer Science, University of Southern California

<sup>3</sup>Department of Computer Science, University of Tokyo

<sup>4</sup>Department of Computer Science, Johns Hopkins University

<sup>5</sup>Department of Biomedical Engineering, Georgia Institute of Technology and Emory University

<sup>6</sup>Department of Radiation Oncology and Winship Cancer Institute, Emory University

## Abstract

Vision-language models (VLMs) have made significant progress in reasoning within natural scenes, yet their potential in medical imaging remains largely under-explored. Medical reasoning tasks, which require robust image analysis and the generation of well-justified answers, present unique challenges due to the inherent complexity of medical images. To be clinically useful, model outputs must be accurate, and logically consistent, as errors or inconsistencies can have critical consequences in medical applications. To address these challenges, we propose Med-R1, a novel framework that investigates whether reinforcement learning (RL) can enhance the generalizability and trustworthiness of VLMs in medical reasoning. Building on the recently introduced DeepSeek strategy, we adopt Group Relative Policy Optimization (GRPO) for RL, which encourages models to explore reasoning paths guided by reward signals. Unlike supervised fine-tuning (SFT), which often overfits to training data and struggles with generalization, RL enables models to develop more robust and diverse reasoning capabilities. We comprehensively evaluate Med-R1 across **eight** distinct medical imaging modalities: Computed Tomography (CT), Magnetic Resonance Imaging (MRI), Ultrasound, Dermoscopy, Fundus Photography, Optical Coherence Tomography (OCT), Microscopy Images, and X-ray Imaging. Compared to the base model, Qwen2-VL-2B, Med-R1 achieves a **29.94%** improvement in average accuracy across these modalities and even outperforms Qwen2-VL-72B—a model with **36 times** more parameters. To assess model’s generalization abilities, we further test on **five** different question types: modality recognition, anatomy identification, disease diagnosis, lesion grading, and biological attribute analysis. Med-R1 also demonstrates superior cross-task generalization, outperforming Qwen2-VL-2B by **32.06%** and Qwen2-VL-72B in question-type generalization accuracy. These results highlight that RL not only enhances medical reasoning capabilities but also enables parameter-efficient models to exceed the performance of significantly larger counterparts. By demonstrating strong cross-domain and cross-tasks performance, Med-R1 points toward a new direction for developing practical and generalizable medical VLMs.

---

\*Equal Contribution

†Corresponding Author: xiaofeng.yang@emory.edu

# 1 Introduction

Vision-language models (VLMs) have achieved remarkable progress in reasoning over natural images (e.g., GPT-4o [16], Gemini-1.5 [33], and Qwen-VL [2]), demonstrating impressive capabilities in tasks such as visual question answering (VQA) and multimodal dialogue. These advancements have been driven by large-scale vision-language pretraining and supervised fine-tuning (SFT), which enables models to associate visual content with textual information. However, applying VLMs to medical imaging reasoning remains a significant challenge. Unlike natural images, medical data demands precise interpretation, requiring VLMs to produce not only answer outcomes but also intermediate reasoning paths that are consistent with clinical decision-making logic. For instance, diagnosing a lung nodule in a CT scan necessitates localizing lesions, analyzing morphological features, and integrating patient history—a reasoning chain that must be both accurate and interpretable to gain clinicians’ trust. Furthermore, the diversity of medical imaging modalities (e.g., CT, MRI, microscopy) and task types (e.g., diagnosis, lesion grading) poses stringent demands on model generalizability. These challenges raise a critical question: How can we equip VLMs with robust reasoning abilities that generalize across medical domains while maintaining medical reliability?

In this paper, we identify that the limitations of current medical VLMs primarily stem from the inherent drawbacks of Supervised Fine-Tuning (SFT) [6, 1]. While SFT has been widely adopted to adapt foundation models to medical imaging [24, 36, 18, 5, 22], it suffers from two fundamental issues that hinder medical applicability. First, SFT inherently biases models toward memorizing task-specific shortcuts rather than learning generalizable reasoning. By directly aligning model outputs with final answers (e.g., diagnostic labels), SFT encourages overfitting to superficial patterns in training data. Second, the scarcity of high-quality Chain-of-Thought (CoT) annotations severely limits the effectiveness of SFT in medical reasoning. Unlike general-domain tasks, where large-scale CoT datasets can be crowdsourced, medical reasoning requires domain-specific logical structuring (e.g., systematically ruling out differential diagnoses before confirming malignancy). However, curating such CoT datasets is prohibitively expensive, as it demands meticulous annotation by experienced medical professionals to ensure diagnostic validity and clinical coherence. As a result, existing SFT-based medical VLMs [24, 36] lack access to high-quality CoT data, leading to shallow and non-clinically grounded reasoning. These models frequently produce "black-box" predictions, struggling to provide traceable reasoning or maintain performance in out-of-domain tasks. This lack of transparency and robustness poses a significant challenge to medical adoption, where explainability and reliability are indispensable requirements.

To address these challenges, we propose Med-R1, a framework leveraging Reinforcement Learning (RL) [29] to enhance both the generalizability and interpretability of medical VLMs. In contrast to SFT, which primarily aligns outputs with fixed supervision, RL promotes exploration of alternative reasoning strategies by leveraging reward-driven feedback, allowing models to construct internal logic without requiring explicit CoT annotations. This approach mitigates overfitting and shortcut learning, as demonstrated by Chu *et al.* [9], who showed that RL-trained vision-language models significantly outperform SFT in cross-domain generalization. Building on recent advancements in RL optimization, we adopt Group Relative Policy Optimization (GRPO) [30], a novel strategy that eliminates the need for complex value models required by traditional methods like Proximal Policy Optimization (PPO) [29]. GRPO incorporates rule-based rewards derived from medical guidelines (e.g., diagnostic criteria for tumors) and group-relative comparisons to stabilize policy updates. For example, rewards can be designed to prioritize reasoning steps that align with radiological decision trees, ensuring clinically plausible rationales. This dual mechanism not only reduces computational overhead but also enforces adherence to domain-specific constraints, making GRPO uniquely suited for medical reasoning tasks where interpretability and scalability are essential for deployment.

As shown in Figure 1, to rigorously validate the effectiveness of Med-R1, we conduct a comprehensive evaluation spanning eight clinically critical imaging modalities: Computed Tomography (CT), Magnetic Resonance Imaging (MRI), Ultrasound, Dermoscopy, Fundus Photography, Optical Coherence Tomography (OCT), Microscopy Images, and X-ray Imaging. These modalities were selected to represent the spectrum of medical imaging challenges, from macroscopic anatomical visualization (CT/MRI) to cellular-level analysis (Microscopy) and functional assessments (OCT). Across these domains, Med-R1 (2B parameters) achieves an average accuracy of 69.91%, representing a 29.94% absolute improvement over its foundation model Qwen2-VL-2B. Notably (Table 2), Med-R1 even surpasses Qwen2-VL-72B—a 72B-parameter model with 36× larger scale, demonstrating that param-

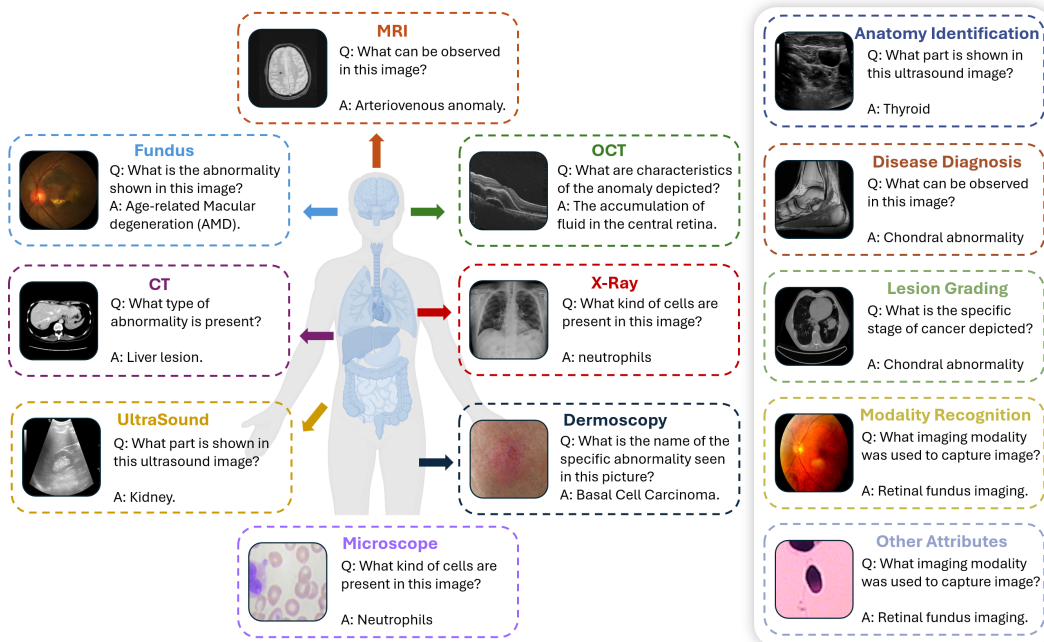


Figure 1: **Overview of the Evaluation Framework: Eight Medical Imaging Modalities and Five Medical Vision Question Answering Tasks.** We evaluate Med-R1 across eight distinct medical imaging modalities—CT, MRI, Ultrasound, Dermoscopy, Fundus Photography, OCT, Microscopy Images, and X-ray Imaging—as well as five medical vision question answering tasks: anatomy identification, disease diagnosis, lesion grading, modality recognition, and biological attribute analysis. Example images and corresponding medical questions illustrate the diversity of medical data and the challenges in developing generalizable vision-language models for automated medical reasoning.

eter efficiency need not compromise performance when leveraging RL-driven reasoning. Beyond evaluating performance across imaging modalities, we also examine Med-R1’s generalizability across different medical question types. We assess the model’s capability in five key question categories: modality recognition, anatomy identification, disease diagnosis, lesion grading, and biological attribute analysis. Med-R1 exhibits superior cross-task generalization, outperforming Qwen2-VL-2B by 32.06% in question-type generalization accuracy, and even surpassing Qwen2-VL-72B in this aspect (Table 4). These findings emphasize the potential of RL-based training in improving both reasoning depth and task adaptability in medical VLMs.

Med-R1 is a generalizable medical VLM that generates interpretable reasoning explanations for medical VQA across eight imaging modalities (Figure 2). We summarized the contribution as follows:

- 1. Generalizable Medical VLM with Multi-Modal Explicit Reasoning:** We propose Med-R1, the first vision-language model supporting **eight medical imaging modalities** (CT, MRI, Ultrasound, etc.), capable of generating step-by-step reasoning explanations without task-specific retraining. Unlike prior SFT-based models limited to single modalities and black-box answers, Med-R1 achieves cross-domain generalization through RL-driven exploration.
- 2. Reward Guided Reasoning via Constrained RL:** We employ **Group Relative Policy Optimization**, a reinforcement learning method that removes the need for explicit reasoning annotations. GRPO combines *rule-informed reward signals* (e.g., alignment with diagnostic protocols) with *group-relative optimization*, allowing models to align output behavior with medically grounded reasoning from final-answer supervision alone.
- 3. Robust and Efficient Generalization:** Med-R1 outperforms the base foundation model by **29.94%** and SFT baselines by **15.84%** in cross-modality performance. It further improves **32.06%** over the foundation model and **11.25%** over SFT baselines on cross-task generalization. Med-R1 also exceeds much larger models in both general-domain and medical-domain settings—including Qwen2-VL-72B and MedVInt-7B—demonstrating scalable reasoning and medical transferability beyond model size.

## 2 Related Works

**General VLMs and Medical VLMs.** VLMs have significantly advanced multimodal understanding by aligning visual and textual representations through large-scale pretraining. General-purpose VLMs, such as CLIP [28] and BLIP-2 [19], excel in natural image-text tasks but encounter challenges when applied to domain-specific medical reasoning. Recent efforts have sought to adapt these models to medical imaging through SFT on domain-specific datasets. For instance, LLaVA [23] introduces instruction tuning for general-purpose vision-language tasks, achieving strong performance on natural image benchmarks. Building on this, LLaVA-Med [18] fine-tunes LLaVA using radiology reports, demonstrating improved performance on medical VQA tasks. Similarly, Med-Flamingo [24] extends Flamingo by incorporating domain-specific pretraining for medical VQA. However, these SFT-based approaches often suffer from overfitting to narrow medical corpora, limiting their generalizability across diverse imaging modalities and medical tasks. Our work addresses this gap by introducing RL for generalization, enabling robust performance without modality-specific retraining.

**Reinforcement Learning for Post-Training.** Reinforcement learning [32, 8] has emerged as a powerful tool for aligning large language models (LLMs) with human preferences through reward signals. Approaches like RLHF [25] and RLAIFF [4] leverage human or AI-generated feedback to refine model behavior. In the vision-language domain, RL has been applied to improve VQA accuracy [9] and reduce hallucination [30]. However, existing methods rely on complex reward models or extensive human annotation, limiting scalability in data-scarce domains like medicine. The Group Relative Policy Optimization addresses these limitations by incorporating rule-based rewards derived from medical guidelines and group-relative comparisons, enabling parameter-efficient adaptation to diverse medical tasks.

**Medical Reasoning and Interpretability** Recent work emphasizes the importance of interpretable reasoning in medical AI, with approaches like CoT prompting [35] and program-guided reasoning [6]. However, acquiring such annotations in the medical domain is particularly challenging due to the need for expert involvement [21], high annotation costs, and the complexity of medical reasoning. The RL approach enables emergent reasoning without explicit supervision, addressing this challenge. Concurrent to our work, MedVLM-R1 [26] explores reinforcement learning for radiology VQA using a GRPO-based approach. While promising, the study is conducted on a small-scale dataset (600 training samples) and does not evaluate generalization across tasks or modalities, which makes it challenging to assess the robustness of the proposed reasoning capability and its generalizability. Nonetheless, this work also reflects the growing interest in applying reinforcement learning to medical vision-language models.

## 3 Method

We adopt RL to encourage multimodal reasoning and generalization in medical domains. Recent studies have demonstrated that RL can incentivize emergent logical reasoning and generalization in multimodal tasks such as mathematical reasoning [15] and visual navigation [9]. Building on these insights, we extend its application to the medical domain and systematically assess its effectiveness in this context. Specifically, we leverage the popular RL-based post-training method GRPO [31] to train a large base MLLM [3] across 8 different modalities for medical reasoning and compare it with zero-shot and SFT performance of popular existing VLMs. We introduce the details of the algorithm, our reward design, and data structure below.

### 3.1 Group Relative Policy Optimization (GRPO)

**Overview.** RL-based algorithms such as PPO [29] and GRPO [30] belong to a family of fine-tuning and alignment strategies explicitly designed to enhance models’ reasoning capacities. Unlike supervised fine-tuning, which directly optimizes maximum likelihood, these RL-based methods instead optimize the policy gradient using reward signals, encouraging reasoning by exploring a much larger solution space. GRPO is closely related to PPO but differs in two key aspects: first, GRPO estimates the advantage using group-based estimation rather than a value function; second, it employs a set of fixed rules as the reward signal instead of a learned reward model. These optimizations make GRPO 50% more resource- and computation-efficient than PPO [30].

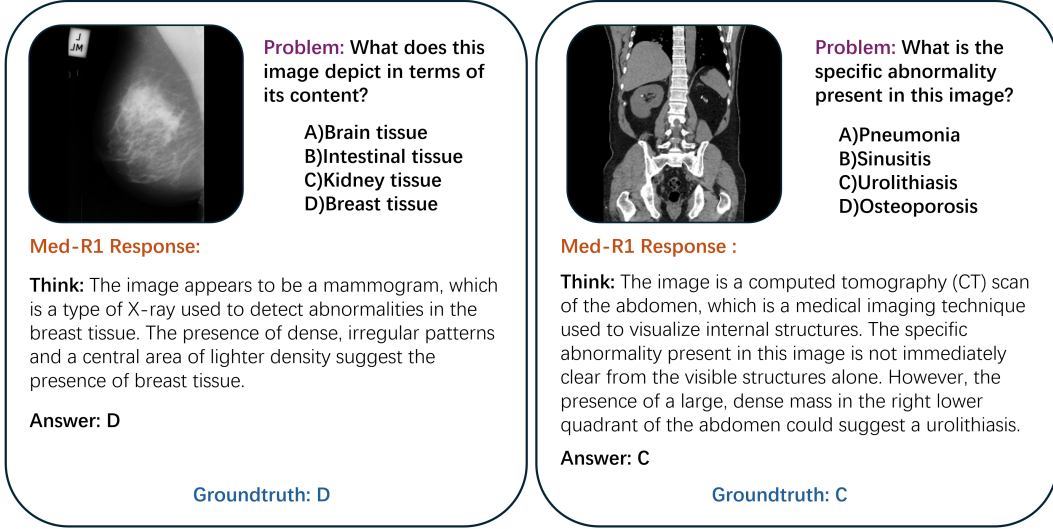


Figure 2: **Medical VQA examples of Med-R1** The left panel demonstrates a modality recognition task, where the model correctly identifies the presence of breast tissue in a mammogram (X-ray). The right panel illustrates a disease diagnosis task, where Med-R1 accurately detects urolithiasis in an abdominal CT scan. In both cases, the model provides interpretable reasoning (“Think”), explaining its decision-making process before selecting the final answer.

**Definition.** Formally, let  $P(Q)$  denote the question set used for training, where  $q$  is a sampled question in the current iteration. Let  $\pi_{\theta_{\text{old}}}$  and  $\pi_{\theta_{\text{new}}}$  denote the old policy and current (new) policy, respectively, where  $o$  is a complete response sampled from a policy. Let  $\pi_{\theta_{\text{ref}}}$  denote the reference policy, which in practice is the frozen base MLLM. Let  $G$  be the number of responses sampled per question in each iteration. The GRPO objective is given by:

$$\mathcal{J}_{\text{GRPO}}(\theta) = \mathbb{E}_{q \sim P(Q), \{o_i\}_{i=1}^G \sim \pi_{\theta_{\text{old}}}(O|q)} \quad (1)$$

$$\frac{1}{G} \sum_{i=1}^G \left( \min \left( \frac{\pi_{\theta_{\text{new}}}(o_i|q)}{\pi_{\theta_{\text{old}}}(o_i|q)} A_i, \text{clip} \left( \frac{\pi_{\theta_{\text{new}}}(o_i|q)}{\pi_{\theta_{\text{old}}}(o_i|q)}, 1 - \epsilon, 1 + \epsilon \right) A_i \right) - \beta \mathbb{D}_{KL}(\pi_{\theta_{\text{new}}} \parallel \pi_{\text{ref}}) \right)$$

where  $\frac{\pi_{\theta}(o_i|q)}{\pi_{\theta_{\text{old}}}(o_i|q)}$  is the policy ratio, and  $A_i$  is the estimated advantage. The KL divergence term [17] regularizes the policy update, ensuring that  $\pi_{\theta}$  does not deviate excessively from the reference model  $\pi_{\theta_{\text{ref}}}$ . Unlike PPO, which uses a critic model to estimate the advantage  $A_i$  for a single response  $o$ , GRPO estimates the relative advantage by sampling a group of responses  $\{o_i\}_{i=1}^G$  and normalizing their rewards within the group to compute a relative advantage [30, 13]. Each reward is calculated based on rules without using a regard model. We detail the reward design below.

**Reward design.** We follow [30] and use two types of reward: format and accuracy. To begin with, we prompt the model to explicitly output its thinking process in the “<think>...</think>” tag and the final answer in the “<answer>...</answer>” tag. The format reward is designed to check if the aforementioned tags are present in the final response. A reward score of 1 will be given if they exist and are correct. This helps the model to organize its thoughts and answer in a structured format for the ease of reading. The accuracy reward is a rule-based reward that checks if the actually answer matches with the ground truth. Similarly, a reward score of 1 is given when the results match. In practice, the ground truths are letter options “A, B, C, D” for multiple choice questions, and we treat all responses with correct letter options as the leading word as correct (“A...”).

### 3.2 No-Thinking-Med-R1

Previous work [20] found that for the image classification task, compared with normal rule-based RL fine-tuning, excluding format accuracy and letting the model only output the final answer could

Table 1: **Cross-Modality Generalization Performance of Med-R1 with RL Post-Training.** Accuracy (%) across eight medical imaging modalities, where rows indicate training modalities and columns test modalities. Darker cell shades indicate higher accuracy for corresponding training-test pairs. The "Overall" column/row reports average performance per training and test domain.

RL fine-tuned VLM									
Train \ Test	CT	MRI	X-Ray	US	Der	FP	OCT	Micro	Overall
<b>CT</b>	98.30	74.43	80.61	51.93	64.17	65.39	70.52	66.13	71.44
<b>MRI</b>	62.33	99.29	73.75	53.18	75.04	64.57	75.59	66.31	71.26
<b>X-Ray</b>	79.67	68.29	95.85	49.32	70.75	76.87	70.28	67.75	72.35
<b>US</b>	55.88	63.96	70.53	99.86	64.78	63.02	63.92	71.53	69.19
<b>Der</b>	53.81	67.36	73.31	49.80	95.10	70.22	64.03	67.93	67.71
<b>FP</b>	54.98	65.95	75.79	49.08	71.36	92.44	65.33	66.40	67.67
<b>OCT</b>	64.48	70.80	77.09	52.65	72.89	73.41	99.17	66.85	72.17
<b>Micro</b>	60.97	63.25	74.92	52.56	64.55	63.66	66.86	93.51	67.54
Overall	66.30	71.67	77.73	57.31	72.33	71.20	71.96	70.80	69.91

CT - Computed Tomography; MRI - Magnetic Resonance Imaging; US - Ultrasound.  
 Der - Dermoscopy; FP - Fundus Photography; OCT - Optical Coherence Tomography  
 Micro - Microscopy Images; X-Ray - X-Ray Imaging

lead to better performance. However, they only discussed this phenomenon for image classification task. In this paper, we further explore the thinking process of medical VQA and propose the No-Thinking-Med-R1.

## 4 Experiment & Results

This section introduces our experimental setup, implementation details, and results.

### 4.1 Setup

**Datasets.** We adopt the VQA data from the open-access part of the OmniMedVQA benchmark [14], which consists of a total of 82,059 images and 88,996 vision question answering pairs. OmniMedVQA includes VQA pairs from eight imaging modalities: CT (15,808), MRI (31,877), X-Ray (7,916), Ultrasound (10,991), Dermoscopy (6,679), Fundus (5,398), OCT (4,646), and Microscopy (5,680). It is also categorized into five VQA question types, including Anatomy Identification (16,448), Disease Diagnosis (55,387), Lesion Grading (2,098), Modality Recognition (11,565), and Other Biological Attributes (3,498). We split the dataset into training and test sets following an 80-20 ratio for each setting.

**Implementation Details** Training is conducted on HGX H100 [7] server with 2xH100 GPUs (80GB VRAM) using PyTorch [27] and FlashAttention-2 [11] for optimized efficiency. We initialize from Qwen2-VL-2B-Instruct [2] with full parameter tuning, employing per-GPU batch size 1 (effective batch size 4 via 2-step gradient accumulation) and bfloat16 mixed precision. Input sequences combine visual embeddings from 328x328 resolution images (max 401k pixels) with textual prompts truncated to 1,024 tokens. The GRPO policy generates four candidate rationales per sample, with a sampling temperature of  $\tau = 0.7$ . Each training configuration is run for one epoch.

**Task setting.** We evaluate our approach in two distinct generalization settings using the OmniMedVQA dataset [14]: cross-modality generalization and cross-task generalization.

- **Cross-modality generalization:** We train our model on a single modality at a time (out of 8 available modalities) and evaluate its performance on the remaining 7 unseen modalities.
- **Cross-task generalization:** We identify 5 distinct task types within the dataset and adopt the same train-test partitioning strategy as in the cross-modality setting, training on one task and evaluating on the remaining four.

Table 2: **Performance Comparison of VLMs on Eight Modality:** Performance comparison across eight medical imaging modalities demonstrates that our GRPO-finetuned model surpasses zero-shot general-purpose VLMs, domain-specific medical VLMs, and conventional supervised fine-tuning approaches, achieving superior accuracy while maintaining scalability for clinical deployment. Meanwhile, in each column, the best and second-best performances are marked in red and blue. Naming details are as follows: CT - Computed Tomography; MRI - Magnetic Resonance Imaging; US - Ultrasound; Der - Dermoscopy; FP - Fundus Photography; OCT - Optical Coherence Tomography; Micro - Microscopy Images; X-Ray - X-Ray Imaging.

Modality Methods	CT	MRI	X-Ray	US	Der	FP	OCT	Micro	Overall
<b>Zero-shot VLM</b>									
BLIP-2 <sup>†</sup> [19]	56.74	41.32	67.58	37.27	40.65	46.24	68.08	50.40	51.04
InstructBLIP <sup>†</sup> [10]	28.72	33.15	61.04	41.25	62.22	50.31	42.59	46.29	45.70
LLaMA Adapter v2 <sup>†</sup> [12]	21.41	26.63	46.44	34.05	51.76	50.74	33.00	38.66	37.83
Qwen2-VL-2B [2]	45.10	38.57	39.32	30.86	35.83	43.17	35.14	36.85	38.11
Qwen2-VL-7B [2]	61.46	45.77	64.27	36.01	49.08	59.84	59.32	61.08	54.60
Qwen2-VL-72B [34]	67.97	69.39	77.21	51.39	65.31	72.58	72.76	67.83	68.05
<b>Zero-shot Medical VLM</b>									
Med-Flamingo <sup>†</sup> [24]	38.47	40.56	30.34	24.64	32.43	30.12	26.51	19.93	30.38
MedVInT <sup>†</sup> [36]	40.74	43.10	55.10	41.26	29.11	31.84	23.26	32.00	37.05
LLaVA-Med <sup>†</sup> [18]	18.69	27.47	30.68	29.88	44.95	39.03	34.61	33.29	32.33
<b>Fine-tuned VLM</b>									
Qwen2-VL-2B (SFT)	51.74	52.83	65.57	47.65	51.91	52.26	53.99	56.58	54.07
<b>Med-R1-2B (GRPO)</b>	66.30	71.67	77.73	57.31	72.33	71.20	71.96	70.80	<b>69.91</b>

**Baseline Methods & Evaluation Metric.** Our evaluation framework integrates three classes of baselines: general VLMs including BLIP-2 [19], InstructBLIP [10], and the Qwen2-VL series (2B/7B/72B) [2, 34]; medical VLMs pretrained on domain-specific corpora (Med-Flamingo [24], MedVInT [36], LLaVA-Med [18]); and SFT variants of Qwen2-VL-2B.

We evaluate model performance using VQA choice accuracy, the standard metric for medical VQA, where models select answers from clinically validated options. Given a medical image  $I$ , a question  $Q$ , and  $K$  candidate answers  $\{A_k\}_{k=1}^K$  (one correct and  $K - 1$  distractors), accuracy is computed as:

$$\text{Accuracy} = \frac{1}{N} \sum_{i=1}^N \mathbb{I}(\hat{y}_i = y_i) \quad (2)$$

where  $N$  is the total number of test cases,  $\hat{y}_i$  is the model’s predicted answer index,  $y_i$  is the ground truth index, and  $\mathbb{I}$  is the indicator function, which returns 1 if the predicted answer matches the ground truth and 0 otherwise.

## 4.2 Cross-Modality Generalization

We comprehensively evaluate Med-R1’s adaptability across **8** medical imaging modalities, including Computed Tomography, Magnetic Resonance Imaging, Ultrasound, Dermoscopy, Fundus Photography, Optical Coherence Tomography, Microscopy Images, and X-ray Imaging. Our experiments focus on two key aspects: (1) cross-modal generalization, where the model is trained on one modality and tested on another, and (2) comparative performance against other popular VLMs and medical-specific VLMs evaluated using zero-shot and SFT.

**Results on generalization.** To evaluate Med-R1’s cross-modality generalization, we measure its accuracy across eight distinct medical imaging modalities (Table 1). The Overall row and column summarize the model’s average performance across training and test domains, providing insights into

Table 3: **Cross-Task Generalization of Med-R1:** Performance is evaluated across five medical reasoning task types (rows: training tasks, columns: test tasks), with darker cell shading indicating stronger generalization. Results demonstrate that domain-specific training (e.g., Disease Diagnosis) preserves in-task expertise while maintaining adaptability to unseen tasks, particularly for modality-agnostic skills like Modality Recognition.

Train \ Test	Anatomy Identification	Disease Diagnosis	Lesion Grading	Modality Recognition	Other Attributes	Overall
Anatomy Identification	96.06	59.07	55.51	98.62	74.86	76.83
Disease Diagnosis	54.16	98.25	73.85	97.87	84.09	81.64
Lesion Grading	52.30	57.72	86.24	97.32	74.29	73.57
Modality Recognition	55.30	55.43	56.88	99.46	70.88	67.59
Other Attributes	56.60	59.93	56.88	97.91	96.59	73.58
Overall	62.88	66.08	65.87	98.24	80.14	74.64

its generalization ability. Med-R1 achieves a strong overall accuracy of 69.91%, demonstrating its ability to generalize across diverse medical imaging modalities. Notably, models trained on CT, MRI, and X-Ray exhibit the highest generalization capability, with overall scores of 71.44%, 71.26%, and 72.35%, respectively. In contrast, models trained on Fundus Photography and Microscopy images show lower generalization, with 67.67% and 67.54% overall accuracy, indicating that certain modality-specific features (e.g., texture-based imaging in US and Micro) may not transfer as effectively to other domains. Importantly, the overall test accuracy of 69.91% highlights Med-R1’s ability to perform well across unseen imaging modalities, despite being trained on a single domain at a time. This result underscores the effectiveness of reinforcement learning in enhancing cross-modality transfer, allowing the model to maintain robust performance without requiring extensive retraining for each medical imaging modality.

**Comparison to zero-shot and SFT evaluations with other VLMs.** As demonstrated in Table 2, Med-R1 demonstrates its superiority across all eight medical imaging modalities while maintaining exceptional parameter efficiency. For zero-shot results, each cell denotes the zero-shot evaluation accuracy of the model on the particular modality. For the fine-tuned VLM results (last two rows), each cell represents the overall accuracy, reflecting the average generalization performance of the given modality when evaluated using models that were separately fine-tuned on each of the eight training modalities. Against general-purpose VLMs, our 2B-parameter model achieves 69.91% overall accuracy, surpassing the 72B-parameter Qwen2-VL by 1.86%—a notable result given the  $36\times$  parameter disparity. This advantage amplifies in critical diagnostic tasks: Med-R1 attains 71.67% accuracy in MRI compared to Qwen2-VL-72B’s 69.39%, and achieves 72.33% versus 65.31% in dermatology, challenging the prevailing scale-equals-performance paradigm. The limitations of specialized medical VLMs become evident through Med-Flamingo’s 30.38% average accuracy, which Med-R1 outperforms by 39.53%. This stark contrast underscores the ineffectiveness of narrow medical pretraining compared to our RL-driven adaptation strategy. When compared to supervised fine-tuning approaches, GRPO delivers 15.84% accuracy gains over SFT-tuned Qwen2-VL-2B (69.91% vs. 54.07%), with particularly significant improvements in CT interpretation (66.30% vs. 51.74%) and OCT analysis (71.96% vs. 53.99%).

### 4.3 Cross-Task Generalization

We also evaluate Med-R1’s generalization across 5 important medical tasks [14]: Anatomy Identification, Disease Diagnosis, Lesion Grading, Modality Recognition, and Other Attributes. Similar to subsection 4.2, we focus our evaluation on two aspects: cross-modality generalization and comparison against SFT and zero-shot with other VLMs.

**Results on generalization.** As shown in Table 3, models trained on “disease diagnosis” data achieve the best generalization, with 81.64% overall accuracy. This suggests that disease diagnosis encompasses diverse feature representations that transfer well across tasks, likely due to its reliance on both anatomical and pathological cues. In contrast, models trained on “modality recognition” exhibit strong generalization in task-agnostic settings (98.24% in the “modality recognition” column), indicating that learning modality distinctions aids in extracting transferable image features. However, training



Table 4: **Performance Comparison of VLMs on Five Medical VQA Tasks:** GRPO Fine-Tuning Outperforms Zero-Shot and SFT Baselines Across Diverse Reasoning Tasks. Performance is evaluated on five medical reasoning types (columns) across three model categories: general-purpose VLMs (zero-shot), medical VLMs (zero-shot), and fine-tuned VLMs (SFT vs. GRPO). Results demonstrate that our compact GRPO-tuned 2B model surpasses even 36× larger zero-shot models and achieves stronger cross-task generalization compared to SFT. Meanwhile, in each column, the best and second-best performances are marked in red and blue.

Types Methods	Anatomy Identification	Disease Diagnosis	Lesion Grading	Modality Recognition	Other Attributes	Overall
<b>Zero-shot VLM</b>						
BLIP-2 <sup>†</sup> [19]	44.39	44.51	29.03	68.19	67.95	48.12
InstructBLIP <sup>†</sup> [10]	44.35	32.29	59.25	75.27	23.72	40.40
LLaMA Adapter v2 <sup>†</sup> [12]	33.72	31.19	41.99	37.29	34.22	32.82
Qwen2-VL-2B [2]	30.70	36.53	43.58	59.90	42.19	42.58
Qwen2-VL-7B [2]	42.57	48.83	52.06	84.74	59.66	57.57
Qwen2-VL-72B [34]	56.41	65.71	62.15	98.11	80.53	72.58
<b>Zero-shot Medical VLM</b>						
Med-Flamingo <sup>†</sup> [24]	24.93	38.90	30.74	30.19	14.18	34.03
MedVInT <sup>†</sup> [36]	40.26	35.78	12.77	68.10	30.30	40.04
LLaVA-Med <sup>†</sup> [18]	29.53	29.22	34.18	26.93	33.08	29.25
<b>Fine-tuned VLM</b>						
Qwen2-VL-2B (SFT)	53.97	51.62	60.71	86.77	63.91	63.39
<b>Med-R1-2B (GRPO)</b>	62.88	66.08	65.87	98.24	80.14	<b>74.64</b>

on “lesion grading” leads to high in-task performance (86.24%) but relatively lower transferability, implying that this task captures more specialized features that do not generalize as effectively. These results highlight the trade-off between specialization and adaptability, emphasizing the importance of task selection when designing models for broad medical applications.

**Comparison to zero-shot and SFT evaluations with other VLMs.** Table 4 shows the comparison results with other popular VLMs evaluated with zero-shot and SFT. For zero-shot results, each cell denotes the zero-shot evaluation accuracy of the model on the particular task. For the fine-tuned VLM results (last two rows), each cell represents the overall accuracy, reflecting the average generalization performance of the given task when evaluated using models that were separately fine-tuned on each of the five training tasks. First of all, the results clearly show that Med-R1 outperforms all other popular VLMs’ zero-shot generalization. Remarkably, Med-R1 even outperforms Qwen2-VL-72B (74.64% vs. 72.58%), a model with **70 billion** more parameters. More importantly, this suggests that RL can effectively elevate small models with moderate capacity, opening doors for many real-world applications where resource is a constraint. In contrast, the average generalization with the identical base model trained with SFT is merely 63.39%, 11.25% below Med-R1, further demonstrating the strong generalization capability of Med-R1.

## 5 Conclusion

In this work, we introduce Med-R1, a RL-enhanced VLM designed to improve medical reasoning across diverse imaging modalities. By leveraging GRPO, Med-R1 effectively overcomes the limitations of SFT, significantly enhancing both cross-modality and cross-task generalization. Comprehensive evaluations across eight medical imaging modalities and five medical reasoning tasks demonstrate that Med-R1 consistently outperforms baseline models, including zero-shot general-purpose VLMs, specialized medical VLMs, and even larger-scale models.

Despite its compact 2B parameter size, Med-R1 achieves competitive performance against 36× larger models, demonstrating that scalability does not have to come at the cost of efficiency. Its lightweight

nature significantly lowers computational and deployment barriers, making it more practical for real-world clinical applications where resource constraints are critical.

While VLM medical reasoning remains an emerging field with ongoing challenges, Med-R1 highlights the potential of reinforcement learning in developing safer, more transparent, and clinically reliable AI-driven healthcare solutions. Future research could further enhance Med-R1 by integrating additional multi-modal medical data, improving uncertainty quantification, and refining expert-aligned interpretability, ultimately advancing scalable and trustworthy medical reasoning systems.

## 6 Acknowledgement

This work is supported in part by the National Institutes of Health under award numbers R01CA272991, R01EB032680, R01DE033512, and U54CA274513.

## References

- [1] J. Achiam, S. Adler, S. Agarwal, L. Ahmad, I. Akkaya, F. L. Aleman, D. Almeida, J. Altenschmidt, S. Altman, S. Anadkat, et al. Gpt-4 technical report. *arXiv preprint arXiv:2303.08774*, 2023.
- [2] J. Bai, S. Bai, Y. Chu, Z. Cui, K. Dang, X. Deng, Y. Fan, W. Ge, Y. Han, F. Huang, et al. Qwen technical report. *arXiv preprint arXiv:2309.16609*, 2023.
- [3] S. Bai, K. Chen, X. Liu, J. Wang, W. Ge, S. Song, K. Dang, P. Wang, S. Wang, J. Tang, H. Zhong, Y. Zhu, M. Yang, Z. Li, J. Wan, P. Wang, W. Ding, Z. Fu, Y. Xu, J. Ye, X. Zhang, T. Xie, Z. Cheng, H. Zhang, Z. Yang, H. Xu, and J. Lin. Qwen2.5-vl technical report, 2025.
- [4] Y. Bai, S. Kadavath, S. Kundu, A. Askell, J. Kernion, A. Jones, A. Chen, A. Goldie, A. Mirhoseini, C. McKinnon, et al. Constitutional ai: Harmlessness from ai feedback. *arXiv preprint arXiv:2212.08073*, 2022.
- [5] J. Chen, C. Gui, R. Ouyang, A. Gao, S. Chen, G. H. Chen, X. Wang, R. Zhang, Z. Cai, K. Ji, et al. Huatuoqpt-vision, towards injecting medical visual knowledge into multimodal llms at scale. *arXiv preprint arXiv:2406.19280*, 2024.
- [6] W. Chen, X. Ma, X. Wang, and W. W. Cohen. Program of thoughts prompting: Disentangling computation from reasoning for numerical reasoning tasks. *arXiv preprint arXiv:2211.12588*, 2022.
- [7] J. Choquette. Nvidia hopper h100 gpu: Scaling performance. *IEEE Micro*, 43(3):9–17, 2023.
- [8] P. F. Christiano, J. Leike, T. Brown, M. Martic, S. Legg, and D. Amodei. Deep reinforcement learning from human preferences. *Advances in neural information processing systems*, 30, 2017.
- [9] T. Chu, Y. Zhai, J. Yang, S. Tong, S. Xie, D. Schuurmans, Q. V. Le, S. Levine, and Y. Ma. Sft memorizes, rl generalizes: A comparative study of foundation model post-training. *arXiv preprint arXiv:2501.17161*, 2025.
- [10] W. Dai, J. Li, D. Li, A. M. H. Tiong, J. Zhao, W. Wang, B. Li, P. Fung, and S. Hoi. Instructblip: Towards general-purpose vision-language models with instruction tuning, 2023.
- [11] T. Dao. Flashattention-2: Faster attention with better parallelism and work partitioning. *arXiv preprint arXiv:2307.08691*, 2023.
- [12] P. Gao, J. Han, R. Zhang, Z. Lin, S. Geng, A. Zhou, W. Zhang, P. Lu, C. He, X. Yue, et al. Llama-adapter v2: Parameter-efficient visual instruction model. *arXiv preprint arXiv:2304.15010*, 2023.
- [13] D. Guo, D. Yang, H. Zhang, J. Song, R. Zhang, R. Xu, Q. Zhu, S. Ma, P. Wang, X. Bi, et al. Deepseek-r1: Incentivizing reasoning capability in llms via reinforcement learning. *arXiv preprint arXiv:2501.12948*, 2025.

- [14] Y. Hu, T. Li, Q. Lu, W. Shao, J. He, Y. Qiao, and P. Luo. Omnimedvqa: A new large-scale comprehensive evaluation benchmark for medical lvlm. In *Proceedings of the IEEE/CVF Conference on Computer Vision and Pattern Recognition*, pages 22170–22183, 2024.
- [15] W. Huang, B. Jia, Z. Zhai, S. Cao, Z. Ye, F. Zhao, Z. Xu, Y. Hu, and S. Lin. Vision-rl: Incentivizing reasoning capability in multimodal large language models, 2025.
- [16] A. Hurst, A. Lerer, A. P. Goucher, A. Perelman, A. Ramesh, A. Clark, A. Ostrow, A. Welihinda, A. Hayes, A. Radford, et al. Gpt-4o system card. *arXiv preprint arXiv:2410.21276*, 2024.
- [17] S. Kullback and R. A. Leibler. On information and sufficiency. *Annals of Mathematical Statistics*, 22(1):79–86, 1951.
- [18] C. Li, C. Wong, S. Zhang, N. Usuyama, H. Liu, J. Yang, T. Naumann, H. Poon, and J. Gao. Llava-med: Training a large language-and-vision assistant for biomedicine in one day. *Advances in Neural Information Processing Systems*, 36:28541–28564, 2023.
- [19] J. Li, D. Li, S. Savarese, and S. Hoi. Blip-2: Bootstrapping language-image pre-training with frozen image encoders and large language models. In *International conference on machine learning*, pages 19730–19742. PMLR, 2023.
- [20] M. Li, S. Zhao, J. Zhong, Y. Lai, and K. Zhang. Cls-rl: Image classification with rule-based reinforcement learning. *arXiv preprint arXiv:2503.16188*, 2025.
- [21] W. Li, C. Qu, X. Chen, P. R. Bassi, Y. Shi, Y. Lai, Q. Yu, H. Xue, Y. Chen, X. Lin, et al. Abdomenatlas: A large-scale, detailed-annotated, & multi-center dataset for efficient transfer learning and open algorithmic benchmarking. *Medical Image Analysis*, 97:103285, 2024.
- [22] Y. Li, Y. Lai, M. Thor, D. Marshall, Z. Buchwald, D. S. Yu, and X. Yang. Towards universal text-driven ct image segmentation. *arXiv preprint arXiv:2503.06030*, 2025.
- [23] H. Liu, C. Li, Q. Wu, and Y. J. Lee. Visual instruction tuning. *Advances in neural information processing systems*, 36:34892–34916, 2023.
- [24] M. Moor, Q. Huang, S. Wu, M. Yasunaga, Y. Dalmia, J. Leskovec, C. Zakka, E. P. Reis, and P. Rajpurkar. Med-flamingo: a multimodal medical few-shot learner. In *Machine Learning for Health (ML4H)*, pages 353–367. PMLR, 2023.
- [25] L. Ouyang, J. Wu, X. Jiang, D. Almeida, C. Wainwright, P. Mishkin, C. Zhang, S. Agarwal, K. Slama, A. Ray, et al. Training language models to follow instructions with human feedback. *Advances in neural information processing systems*, 35:27730–27744, 2022.
- [26] J. Pan, C. Liu, J. Wu, F. Liu, J. Zhu, H. B. Li, C. Chen, C. Ouyang, and D. Rueckert. Medvlm-rl: Incentivizing medical reasoning capability of vision-language models (vlms) via reinforcement learning. *arXiv preprint arXiv:2502.19634*, 2025.
- [27] A. Paszke, S. Gross, F. Massa, A. Lerer, J. Bradbury, G. Chanan, T. Killeen, Z. Lin, N. Gimelshein, L. Antiga, et al. Pytorch: An imperative style, high-performance deep learning library. *Advances in neural information processing systems*, 32:8026–8037, 2019.
- [28] A. Radford, J. W. Kim, C. Hallacy, A. Ramesh, G. Goh, S. Agarwal, G. Sastry, A. Askell, P. Mishkin, J. Clark, et al. Learning transferable visual models from natural language supervision. In *International conference on machine learning*, pages 8748–8763. PmLR, 2021.
- [29] J. Schulman, F. Wolski, P. Dhariwal, A. Radford, and O. Klimov. Proximal policy optimization algorithms. *arXiv preprint arXiv:1707.06347*, 2017.
- [30] Z. Shao, P. Wang, Q. Zhu, R. Xu, J. Song, X. Bi, H. Zhang, M. Zhang, Y. Li, Y. Wu, et al. Deepseekmath: Pushing the limits of mathematical reasoning in open language models. *arXiv preprint arXiv:2402.03300*, 2024.
- [31] Z. Shao, P. Wang, Q. Zhu, R. Xu, J. Song, X. Bi, H. Zhang, M. Zhang, Y. K. Li, Y. Wu, and D. Guo. Deepseekmath: Pushing the limits of mathematical reasoning in open language models, 2024.

- [32] D. Silver, J. Schrittwieser, K. Simonyan, I. Antonoglou, A. Huang, A. Guez, T. Hubert, L. Baker, M. Lai, A. Bolton, et al. Mastering the game of go without human knowledge. *nature*, 550(7676):354–359, 2017.
- [33] G. Team. Gemini 1.5: Unlocking multimodal understanding across millions of tokens of context, 2024.
- [34] P. Wang, S. Bai, S. Tan, S. Wang, Z. Fan, J. Bai, K. Chen, X. Liu, J. Wang, W. Ge, et al. Qwen2-vl: Enhancing vision-language model’s perception of the world at any resolution. *arXiv preprint arXiv:2409.12191*, 2024.
- [35] J. Wei, X. Wang, D. Schuurmans, M. Bosma, F. Xia, E. Chi, Q. V. Le, D. Zhou, et al. Chain-of-thought prompting elicits reasoning in large language models. *Advances in neural information processing systems*, 35:24824–24837, 2022.
- [36] X. Zhang, C. Wu, Z. Zhao, W. Lin, Y. Zhang, Y. Wang, and W. Xie. Pmc-vqa: Visual instruction tuning for medical visual question answering. *arXiv preprint arXiv:2305.10415*, 2023.